JTTEES 7:97-107

PEER REVIEWED

# Parameter Study of HP/HVOF Deposited WC-Co Coatings

*H.L. de Villiers Lovelock, P.W. Richter, J.M. Benson, and P.M. Young*

*(Submitted 19 December 1996; in revised form 22 October 1997)*

**The deposition parameters of WC-17%Co coatings produced using the JP-5000 liquid-fuel HP/HVOF system (Eutectic TAFA) were investigated with the initial purpose of parameter improvement and optimization. The coating microstructures, porosities, phase compositions, and abrasion resistance were characterized. Preliminary work using the Taguchi statistical experimental design method aimed at optimizing the spray parameters in terms of the microstructure and phase composition was unsuccessful. The variations in the measured properties were too small to be correlated with the spray parameters. Subsequent experiments showed this was primarily due to the fact that the properties, particularly the abrasion resistance, of the WC-Co coatings were not primarily influenced by variations in the spray parameters, but were more dependent on the powder composition, particle size range, and manufacturing route. Hence, the application of Taguchi techniques would have been more effective over a much wider parameter space than was originally used. This result is valuable because it suggests that this process is robust and can be used for WC-Co coatings without large investments in spray parameter optimization and control once the coating and powder type have been fixed.**

**Keywords** abrasion tests, HVOF process, process optimization, WC-Co coatings

## 1. Introduction

For most thermal spray processes, the optimization of the spray parameters is not a trivial task. This is due primarily to the large number of processing parameters or factors involved. Plasma and gas-fuel high velocity oxygen fuel (HVOF) spray parameters have been successfully optimized using statistical design of experiment (DOE) techniques (Ref 1, 2), particularly the Taguchi method (Ref 3-6), but no results have been published for liquid fuel HVOF processes. The original purpose of this study was to determine whether the Taguchi method could be used for the optimization of the liquid fuel high performance/high velocity oxygen fuel (HP/HVOF) process. The Taguchi method is briefly introduced.

The Taguchi method, first used in the 1940s by Dr. G. Taguchi, and based on the DOE methods of Sir Ronald Fisher, makes use of orthogonal arrays to design an experimental matrix which enables the use of statistical methods to evaluate the effects of different experimental variables simultaneously. This drastically reduces the number of experiments which would otherwise be required to optimize a process. The method involves the following steps.

### 1.1 *Brainstorming*

Some experience of the process is required for the Taguchi method to be successful. Using this experience base, the most important process variables, or factors, are identified by a team of people. Two or more levels at which each factor will be set for the purpose of the experiment are determined. At this stage the process output variables, or responses, which one is trying to optimize (for example coating porosity), are defined.

**H.L. de Villiers Lovelock, P.W. Richter, J.M. Benson, and P.M. Young,** MATTEK, CSIR, P.O. Box 395, Pretoria, 0001, South Africa

### 1.2 *Experiments*

A specialist, familiar with the Taguchi approach, uses the chosen factor levels and draws up an experimental matrix dictating the combinations of the levels at which the factors should be set for each experiment that is to be conducted. The experiments are conducted randomly to minimize the effect of systematic errors. Each experiment is preferably repeated one or more times.

### 1.3 *Analysis*

The Taguchi specialist conducts statistical analysis on the results, that is an effects analysis and analysis of variance (ANOVA), to determine the relative contributions of the various main factors and interactions among them. A prediction is then able to be made as to the process settings which will produce an optimum result, and this can be tested in subsequent confirmation runs.

In the work described here, the Taguchi method was applied to the liquid fuel HP/HVOF process for the spraying of WC-17%Co coatings. Based on the results obtained, further work was performed to verify certain points.

## 2. Experimental Techniques

### 2.1 *Spray Parameter Selection for the Taguchi Analysis*

The parameters used for the Taguchi experimental design are shown in Tables 1(a and b), and the powders are detailed in Table 2. An L16 orthogonal array was used in the design of

the experiments. Since the aim of the study was to see whether the Taguchi approach could be potentially useful for this process, no replications were done. The use of an L16 array with nine factors does not allow for Resolution IV design. In the design the main factors were assigned to columns 1, 2, 4, 7, 8, 11, 13, 14, and 15 of the L16 orthogonal array, with various interactions assigned to the remaining columns. Column 7 was originally assigned to the variable "gun barrel length." However, the 8 in. barrel consistently clogged with powder during spraying. This column was reassigned to an interaction, and the variable "bar-

**Table 1(a) Main experimental factors and their levels used for the Taguchi experimental design**

| Parameter | Baseline used | Low level (1) | High level (2) |
|---|---|---|---|
| Spray system | JP-5000 system, 4 in. spray barrel, Miller Rotofeed 1270 powder feeder | ... | ... |
| Combustion pressure, kPa (psi) | 711 to 773 (103 to 112) | ... | ... |
| Oxygen supply pressure, kPa (psi) | 1450 (210) | ... | ... |
| Cooling water flow rate, L/min (gph) | 0.38 (6) | ... | ... |
| Kerosene flow rate, L/min (fuel) (gph) | 0.347 (5.5) | 0.328 (5.2) | 0.365 (5.8) |
| $O_2$/fuel ratio, scfh/gph (resulting scfh $O_2$) | ... | 328 (1705, 1900) | 385 (1925, 2235) |
| Spray distance, mm | 380 | 370 | 390 |
| Spray angle to surface | 90° | 60° | 90° |
| Preheat pass | None | None | One |
| Powder source | N/A | Amperit 526.074 | TAFA 1343V |
| Powder feed, g/min (approx. feeder wheel speed, rpm) | 150 (10) | 120 (8) | 170 (11.5) |
| Powder carrier gas, L/min | 26 | 23 | 29 |
| Traverse speed, step size | 375 mm/s, 5 mm | ... | ... |

**Table 1(b) Experimental matrix used for the Taguchi experimental design**
**1 indicates factor set at low level; 2 indicates factor set at high level**

| Run No.:→ | 1 | 2 | 3 | 4 | 5 | 6 | 7 | 8 | 9 | 10 | 11 | 12 | 13 | 14 | 15 | 16 |
|---|---|---|---|---|---|---|---|---|---|---|---|---|---|---|---|---|
| **Factor:↓** | | | | | | | | | | | | | | | | |
| Kerosene flow | 1 | 2 | 1 | 2 | 1 | 2 | 1 | 2 | 1 | 2 | 1 | 2 | 1 | 2 | 1 | 2 |
| $O_2$/fuel flow ratio, scfh/gph | 1 | 1 | 1 | 1 | 1 | 1 | 1 | 1 | 2 | 2 | 2 | 2 | 2 | 2 | 2 | 2 |
| Spray distance | 1 | 2 | 2 | 1 | 1 | 2 | 2 | 1 | 2 | 1 | 1 | 2 | 2 | 1 | 1 | 2 |
| Spray angle | 1 | 2 | 2 | 1 | 2 | 1 | 1 | 2 | 1 | 2 | 2 | 1 | 2 | 1 | 1 | 2 |
| Preheat pass | 2 | 1 | 1 | 2 | 1 | 2 | 2 | 1 | 1 | 2 | 2 | 1 | 2 | 1 | 1 | 2 |
| Powder type | 1 | 2 | 1 | 2 | 2 | 1 | 2 | 1 | 2 | 1 | 2 | 1 | 1 | 2 | 1 | 2 |
| Powder feed | 1 | 1 | 1 | 1 | 2 | 2 | 2 | 2 | 1 | 1 | 1 | 1 | 2 | 2 | 2 | 2 |
| Carrier gas | 1 | 1 | 2 | 2 | 1 | 1 | 2 | 2 | 1 | 1 | 2 | 2 | 1 | 1 | 2 | 2 |

**Table 2 Powders used for the Taguchi experimental design**

| | Agglomerated (Type 1) | Agglomerated (Type 2) | Sintered crushed (Type 3) |
|---|---|---|---|
| Nominal composition | WC 17%Co | WC 17%Co | WC 17%Co |
| Trade name | Amperit 526.074 | TAFA 1343V | WC-516 |
| $Carbon_{total}$/$Carbon_{free}$/Co | 5.13%/0.03%/16.66% | 5.16%/0.04%/16.74% | 4.88%/nd/17.32% |
| Average WC size | ≈1.7 μm | ≈2.6 μm | ≈1.0 μm |

nd indicates not determined.

**Table 3 Coating polishing procedure**

| Paper or cloth | Medium | Lubricant | Procedure |
|---|---|---|---|
| SiC No. 220 paper | ... | Water | 10 min, 300 rpm, → rotation mode, 120 N force (6 specimens) |
| Struers DP-Plan (nylon) | 9 μm diamond | Blue | 5 min, 150 rpm, → rotation mode, 150 N force (6 specimens) |
| Struers DP-Dur (silk) | 3 μm diamond | Blue | 5 min, 150 rpm, → rotation mode, 150 N force (6 specimens) |
| Struers OP-Chem | OP-U | ... | 2 min, 150 rpm, ↔ rotation mode, 100 N force (6 specimens) |

Rotation mode, → is same direction. ↔ is counter direction.

rel length" was abandoned. Nevertheless for all of these columns except column 14 (which was assigned to the factor "spray angle"), no confounding of the main factors with two-way interactions of other factors will occur; although there may be confounding interactions of two-way interactions. The effect was expected to be small and therefore to allow the influence of the main factors to be determined without too much interference from interactions.

The experimental runs of a given design were performed in random order to reduce the influence of potential systematic errors. Due to cost and time constraints, no replications of any given trial were done, except for those discussed in section 4, but a conservative estimate of the error variance could be obtained by pooling the sum of squares of the factors that were found to have a small (<2%) contribution or small F-ratio from the ANOVA. Pooling was done until the degrees of freedom of the error term were approximately half that of the total number of degrees of freedom. The Qualitek 4 commercial software package for Taguchi design of experiments (Nutek Inc., Birmingham, MI) was used to facilitate analysis of the results.

### 2.2 *Powder and Coating Evaluation*

The powder morphology was examined using the scanning electron microscope (SEM). The average WC size in the powder particles was estimated using a graphical method, taking into account about one hundred WC particles in a mounted and polished powder cross section (Ref 7). The particle size distributions were compared using the laser-light scattering method (Malvern "Mastersizer" system).

X-ray diffraction (XRD) from 20 to 100° 2θ using $Cu_\alpha$ radiation, a step size of 0.02°, and a fixed time of 2 s per step was conducted on the powders as well as the coatings. The amount of amorphous content in each coating was evaluated qualitatively by ranking the coatings in terms of the size of the amorphous "hump" seen on the XRD spectrum.

The coatings produced were sectioned using a Struers Unitom cutting machine with a low cutting feed rate, mounted in hot-setting clear resin, ground, and polished on a semiautomatic polishing machine (Struers Rotopol/Pedemat; Struers) using the procedure shown in Table 3. The porosity and coating thickness were both determined using a KONTRON IBAS image analyzer system(KONTRON). The microstructures were evaluated using optical microscopy; that is, the distribution of the WC, the degree of visible retention in the cobalt matrix of the carbide phases, and the apparent porosity were noted. A low porosity, the presence of well-distributed retained WC particles, and the absence of cobalt "pools" were treated as the most important attributes, and the microstructures were ranked on a scale from 1 (good) to 5 (bad) for the purposes of analysis.

The deposition efficiencies (DE) of the parameters were compared by measuring the thickness of the material deposited per pass and converting this figure using the following formula to compensate for the use of two different powder feed rates:

$$DE = \text{passes per minute} \times \mu\text{m per pass} \div \text{g per minute} \times 100 \quad \text{(Eq 1)}$$

Ignoring the first term, which is the same for all of the coatings produced in this study, and assuming the same density for all the coatings, a number is obtained that is merely an indication of the thickness deposited per gram of powder fed.

After the Taguchi analysis was completed, subsequent samples were produced (see sections 4 and 5) and evaluated microstructurally and in three-body abrasion wear tests. The dry sand rubber wheel (DSRW) three-body abrasion tests were conducted using the apparatus described in ASTM specification G 65-94. In this test, a flat specimen is pressed against a rotating rubber wheel while sand is fed into the interface between the specimen and the wheel. The method used corresponds to ASTM G 65-94, except that a lower load (50 N) was applied to the specimen/wheel interface, and angular Delmas silica of size 5 to 350 μm, instead of rounded Ottawa silica of size 210 to 300 μm, was used. Samples were weighed at 5 min intervals and the total testing time was 25 min. The wheel rpm was 200 and the diameter 227.5 mm. As is usual for this test, the wear rates were initially high and became reasonably stable after 5 to 10 min. Each result given is the average of tests on two samples.

## 3. Experimental Results and Discussion of Taguchi Analysis

### 3.1 *Powders*

All three powders (Table 2) are nominally 16 to 45 μm in size and are sold for HVOF spraying. Powders 1 and 2 are produced by agglomerating fine WC and Co particles to form a spheroidally shaped powder, followed by size classification and sintering/plasma densification. Powder 3 is produced by sintering fine WC and Co particles to form a porous block of material, followed by crushing and size classification. The powder particle size distributions are shown in Fig. 1. When comparing the size distributions in Fig. 1 to the nominal size, it should be remembered that the results of laser light scattering methods cannot be compared to the results of sieve analysis, for example, since the measurement principles are very different. Laser light scattering is well suited to the accurate comparison of similar powder lots,

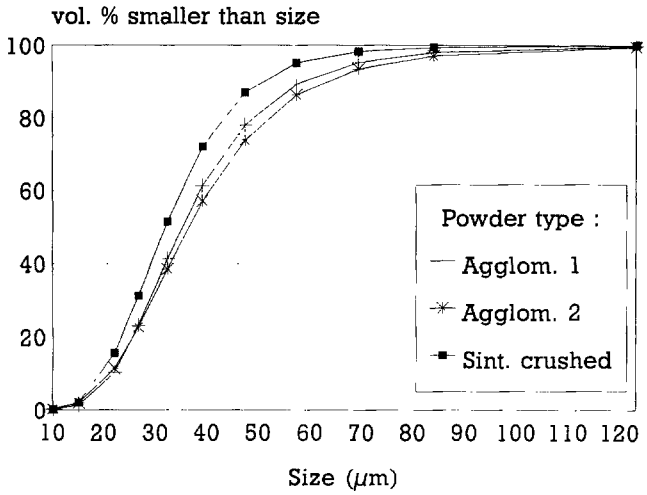


**Fig. 1** Malvern particle size analysis results for the powders used (cumulative distribution)

but tends to overestimate the percentage of coarser particles in a powder (Ref 8). In this case, the results show that the agglomerated powders are very similar in size, with powder 1 only slightly finer. The crushed powder is finer than both of the agglomerated powders. The WC size *range* in the powders when examined in cross section was approximately 1 to 10 μm for all of the powders, but the *average* WC size varied as shown in Table 2. The agglomerated powders contained large pores and tended to be partially hollow, while the blocky-shaped crushed powder contained much less porosity. The two agglomerated powders can be considered to be almost identical except for average WC size.

### 3.2 *Coating and Powder Phase Composition*

Results of the XRD analysis of the coatings and powders are summarized in Table 4. The coatings all contained WC as the major phase, with trace amounts of $W_2C$ and W. No ternary W-C-Co phases were detected. The $W_2C$:WC peak height ratio varied between 1.4% and 3.5%, which is not a significant variation. This can be compared with a range of 1 to 16% observed in coatings produced by $Ar/H_2$-plasma spraying. The W:WC peak ratio varied between only 1.8% and 3.8% (1.3% and 5% for APS). The degree of measurable WC decomposition is therefore lower for HVOF than for $ArH_2$-APS coatings, as has been shown by previous studies in this field (Ref 9-15). The amorphous content of the HVOF coatings is, however, significantly large, even when compared to APS coatings. The amorphous matrix usually contains W-Co-C phases, such as $Co_3W_3C$, $Co_6W_6C$, $Co_3W_9C_4$, $Co_2W_4C$, and $Co_2W_4C_4$. These phases are not detectable by XRD due to their nanocrystalline state (Ref 6, 16-21). Evidence of partial recrystallization of the amorphous binder phase by means of nucleation of $Co_xW_yC_z$ crystallites at the WC/Co interface has been documented (Ref 16, 17). The amor-

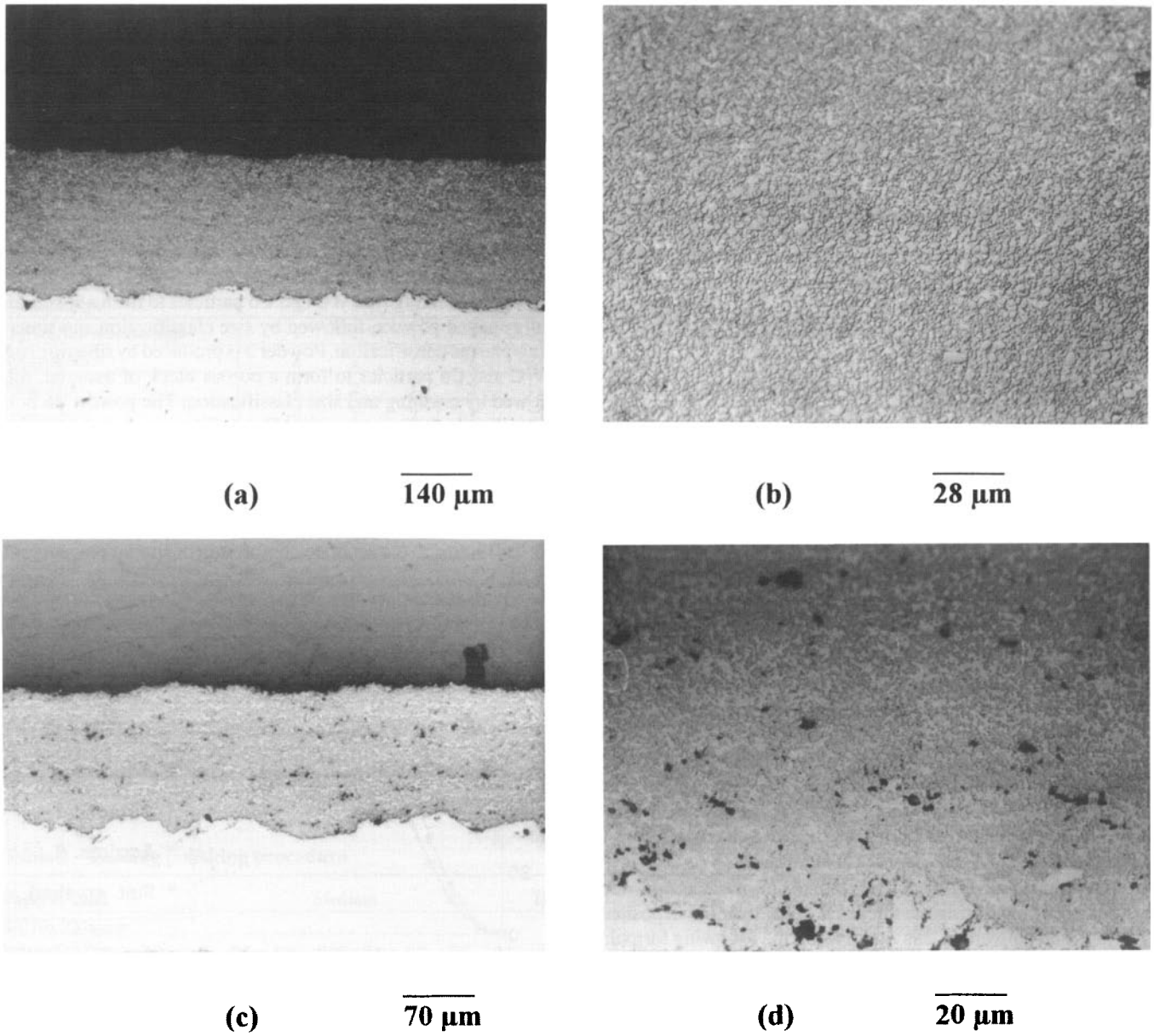


**Fig. 2** Microstructures for HVOF test runs: (a) and (b) Run 10 (L) (one of the best), (c) and (d) Run 7 (F) (one of the worst)

phous Co-W-C binder alloy has also been observed to recrystallize during heat treatment of the coating at about 900 K or be transformed into crystalline $Co_xW_yC_z$ phases detectable by XRD during vacuum or air heat treatment above approximately 1100 K (Ref 15, 18-19). Therefore, due to the presence of the amorphous matrix, it can not be concluded from this work that there is very little WC decomposition in the HVOF coatings.

Whether the formation of non-WC carbide phases is beneficial or detrimental for wear resistance depends on the details of the tribosystem under consideration, and possibly on the detailed coating composition and microstructure, since there are conflicting reports in the literature (Ref 21). Generally however, it is considered detrimental (Ref 12, 14, 22-27) although it appears that in some cases the integrity of the microstructure can affect the wear rates more than the degree of loss of WC (Ref 17). Some HVOF coatings have been observed to perform better than sintered hard metals of comparable composition in mild hydroabrasive wear as well as three-body abrasion (dry sand rubber wheel) tests, and this has been tentatively ascribed to the presence of the nanocrystalline matrix, which is stronger than pure cobalt (Ref 9, 28). Other workers have found coatings to wear at a higher rate than their sintered counterparts (Ref 29).

**Table 4 X-ray diffraction results summary for HVOF sprayed coatings**

| Test No. | $W_2C$ | W | Cobalt hcp | Amorphous content ranking(a) |
|---|---|---|---|---|
| Powder 1 | ... | ... | 4.2 | 0 |
| Powder 2 | ... | ... | 4.3 | 0 |
| 1 (A) | 1.8 | 2.9 | ... | 6 |
| 2 (H) | 3.5 | 2.8 | ... | 8 |
| 3 (J) | 1.8 | 2.8 | ... | 2 |
| 4 (N) | 3.3 | 2.4 | ... | 6 |
| 5 (P) | 2.3 | 2.9 | ... | 5 |
| 6 (K) | 2.2 | 2.7 | ... | 4 |
| 7 (F) | 3 | 2.2 | ... | 7 |
| 8 (C) | 1.8 | 2.8 | ... | 6 |
| 9 (O) | 1.7 | 2.2 | ... | 3 |
| 10 (L) | 1.8 | 1.8 | ... | 2 |
| 11 (G) | 1.9 | 2.2 | ... | 6 |
| 12 (B) | 1.7 | 2.6 | ... | 3 |
| 13 (D) | 1.4 | 2.4 | ... | 4 |
| 14 (E) | 3.4 | 3.8 | ... | 7 |
| 15 (I) | 1.7 | 2.6 | ... | 3 |
| 16 (M) | 2 | 1.9 | ... | 1 |

Numbers indicate the ratio of each phase peak height to the $d = 2.518$ Å WC peak height, times 100. This does *not* represent a percentage. The $d$-values of the peaks used are as follows: for $W_2C$, $d = 2.28$; for $Co_3W_3C$, $d = 2.13$; for $Co_3W_9C_4$, $d = 2.17$; for W, $d = 2.24$; for $CoC_x$, $d = 2.08$; for hcp Co, $d = 2.03$. WC was always the major phase. Phases not listed in this table were not detected. (a) Where 0 is none, and 8 is highest amorphous content observed.

**Table 5 Summarized results of HVOF test runs using L16 matrix**

| Test No. | Porosity, % | XRD(a) | Microstructure(b) | µm per pass | DE factor |
|---|---|---|---|---|---|
| 1 (A) | 1.84 | 6 | 4 | 50 | 42 |
| 2 (H) | <0.02 | 8 | 1 | 43 | 36 |
| 3 (J) | <0.01 | 2 | 1 | 41 | 34 |
| 4 (N) | 0.1 | 6 | 5 | 31 | 26 |
| 5 (P) | 0.16 | 5 | 3 | 46 | 27 |
| 6 (K) | <0.01 | 4 | 2 | 36 | 21 |
| 7 (F) | 0.10 | 7 | 5 | 59 | 35 |
| 8 (C) | 0.18 | 6 | 5 | 51 | 30 |
| 9 (O) | 0.07 | 3 | 1 | 28.5 | 24 |
| 10 (L) | <0.05 | 2 | 1 | 36 | 30 |
| 11 (G) | <0.01 | 6 | 5 | 31 | 26 |
| 12 (B) | 0.89 | 3 | 4 (tendency to clog barrel) | 33 | 28 |
| 13 (D) | 0.39 | 4 | 4 | 65 | 38 |
| 14 (E) | 0.22 | 7 | 5 (barrel clogged at end) | 75 | 44 |
| 15 (I) | <0.02 | 3 | 1 | 52 | 31 |
| 16 (M) | <0.05 | 1 | 1 (barrel clogged at end) | 52 | 31 |

(a) See Table 4 for XRD details. (b) Microstructures are ranked 1 to 5. 1 to 4 are acceptable.

## 3.3 *Results of Taguchi Analysis*

Experimental results for the coatings are summarized in Table 5. Typical microstructures are shown in Fig. 2, and typical XRD curves are shown in Fig. 3.

The microstructures of most of the coatings were good with a low porosity and similar proportions of visible carbide particles in the cross sections. An optimized set of spray parameters would preferably maximize the deposition rate, while obtaining

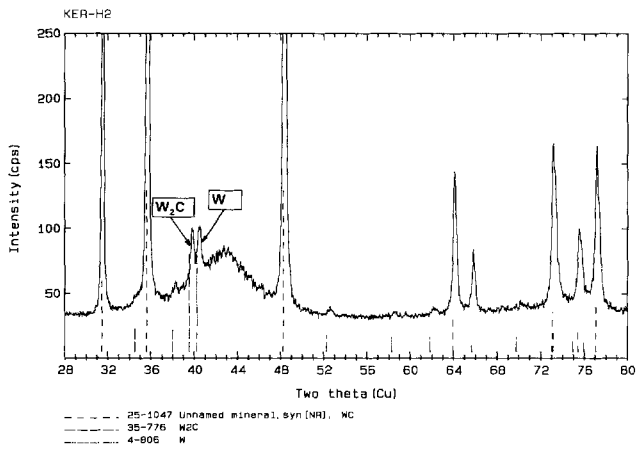


(a)

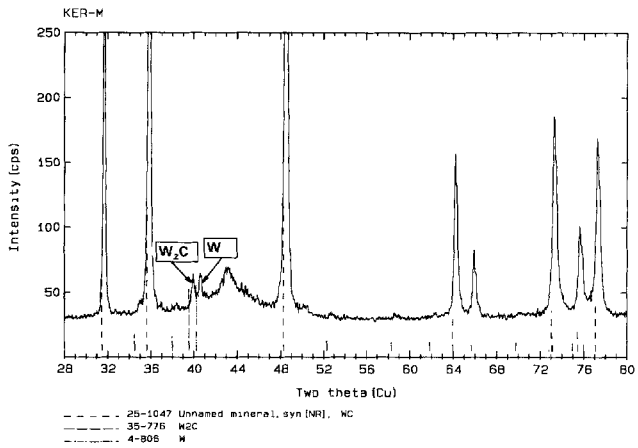


(b)

**Fig. 3** XRD spectra for (a) the highest amorphous content (run 2) and (b) the lowest amorphous content (run 16). The unlabeled peaks represent WC.

a good WC distribution and low porosity in the microstructure, and minimizing the degree of amorphous phase formation as evidenced by the amorphous "hump" in the XRD spectrum. Statistical analysis of the results shown in Table 5 was aimed at identifying the optimum parameters that would achieve this. Upon analyzing the effect of the various spray parameter factors, such as spray distance and powder feed rate, on the individual coating properties shown in Table 5, it was found that various interactions among the factors appeared to have more influence than any single factor. Furthermore, there was a large degree of error. The corresponding predicted optimum spray parameters were nevertheless determined and are shown in Table 6.

The large influence of interactions and error on all of the variables investigated was a matter of concern. This type of effect can be real, or it can be caused by one or more of the following.

#### 3.3.1 The Process Itself Might Not be Repeatable

Significantly different results might be obtained even at the same process settings. If the set level of any factor can not be held constant from run to run, then the effect of its (arbitrary) variation would appear in the analysis. This variation arises from the effect of the change in levels of other factors on this factor; that is, it would appear that the interactions between this factor and others are important, even if they are not. In the first-generation system used here, the kerosene and oxygen flow settings and other variables (for example, kerosene quality) are not as precisely controllable as those in plasma or gas-fuel HVOF systems. For example, the kerosene flowmeter used was marked in graduations of approximately 5 mm (which corresponded to 0.5 gph) with a floating ball approximately 5 mm in diameter. The oxygen flowmeter was marked in graduations of 50 scfh. But the required settings for the experiments (and even for some of the recommended spray parameters from the system manufacturer) were of finer resolution than these meter readings. This could cause a lack of reproducibility, bearing in mind that the spraying was performed by robot and all external variables, such as grit blasting, surface roughness, substrate type, were very closely controlled. Repeat runs of three of the experiments were conducted as described in section 4 and showed that the microstructural and XRD measurements were not reproducible.

**Table 6 Predicted optimum spray parameters**

| Parameter | Best microstructure (set E in Table 7) | Lowest amorphous content (set F in Table 7) | Highest DE (set G in Table 7) |
|---|---|---|---|
| Kerosene, gph | 5.2 | 5.8 | 5.2 |
| $O_2$/fuel ratio, scfh/gph | 385 | 385 | 385 |
| Spray distance, mm | 390 | 390 | 370 |
| Spray angle | 90° | 90° | 90° |
| Preheat | No | Yes | No |
| Powder | Type 1 | Type 1 | Type 1 |
| Powder feed, g/min | 120 | 120 | 170 |
| Powder carrier gas, L/min | 23 | 29 | 23 |

#### 3.3.2 The Chosen Parameter Space Might be too Small

This lack of space would lead to the variations observed in the coating properties being (a) possibly due more to process variability than to the chosen parameters and (b) possibly too small to be of significance. To test this, the follow-up work described in section 5 used as wide a range of spray parameters as possible, and the results confirm this hypothesis.

#### 3.3.3 The Observed Variations in Coating Characteristics Might Not be Large Enough to be Significant

For example, from a practical viewpoint (e.g. wear rate) the fact that the porosity varies between 0.01 and 1.84% was treated as significant in the Taguchi study, but may in fact be insignificant. Hence, it was decided to conduct wear tests, and not only microstructural studies, in the follow-up work described in sections 4 and 5.

#### 3.3.4 The Error in the Measurement of Some of the Properties, Particularly Porosity, can be too Large Relative to the Actual Magnitude of the Property

This was checked by repeating the porosity measurements, as described in section 4. The effect of metallographic preparation was also investigated. Results show that although the measured percentage porosity varies between 0.01 and 0.89, each measurement is only accurate to within 0.4. The XRD and DE results are, however, believed to be accurate and were not repeated.

## 4. Results of Initial Confirmation Runs and Replications

### 4.1 *Samples Sprayed*

Based on the above observations, runs 1, 6, and 10 in Table 5 were repeated to check on reproducibility. Simultaneously the predicted optimum runs shown in Table 6 were also sprayed. Table 7 summarizes the parameters used for these coatings, with parameter sets A, B, and C being the repeats, and set D being the original starting or baseline parameter. In addition to using the agglomerated powder, these confirmation runs were conducted using a sintered and crushed powder to obtain an indication of the effect of using a different powder.

The samples obtained were evaluated in the same manner as the previous samples but were also subjected to the abrasion test described in section 2.1.

### 4.2 *Accuracy of Porosity Measurements*

The porosity was measured as an average of ten measurements for each sample. To determine the reproducibility of the porosity measurements, each series of measurements was first repeated without repolishing the samples. The results indicated an accuracy of only approximately 0.4; that is, a measurement of 1.3% porosity should be read as $1.3 \pm 0.4$.

Subsequent to this, to identify possible effects of metallographic preparation, the porosity was first measured. Samples were ground back an additional 1.5 mm, and then the porosity

was remeasured, after which they were ground down an additional 1.5 mm and remeasured. It was found that the porosity is initially high and then stabilizes at a more or less constant value. It is necessary to grind samples down by at least 2 to 3 mm in order to ensure that any damage induced by sectioning is removed and the true microstructure is revealed. Based on this result, the porosities of runs 1, 6, and 10 of the initial experimental coatings (Table 5) were again measured after repolishing, but the results (all of them were 0.2%) still showed no correlation with those shown in Table 8. In Tables 8 and 9, the decrease in porosity/pullout after repolishing is clearly demonstrated.

### 4.3 *Other Coating Properties*

Most of the results for the repeat runs (Tables 8-11) differ from the original runs. This could be due to any or all of the reasons mentioned in section 3.3.1 to 3.3.4. As shown in Fig. 4, there is a correlation between the microstructure ranking as qualitatively evaluated in cross section and the amorphous content ranking based on the XRD spectrum. As the amorphous content (the WC decomposition) in the coating increases, the microstructure tends to get worse. The same tendency is observed for the sintered and crushed powder coatings, but their microstructures tend to be worse. Furthermore, their XRD results are better than for the other coatings.

### 4.4 *Abrasion Rate*

The average steady-state wear rate is about 40% higher for coatings produced from the agglomerated powders than for those produced from the sintered and crushed powders, while total wear mass loss is approximately 17% higher. Hence, powder type and/or size could be a major contributing factor to the

**Table 7 Spray parameters used in confirmation runs and subsequent experiments**

| Set No. | Kerosene flow rate, gph | $O_2$ flow rate, scfh | Spray distance, mm | Spray angle | Preheat pass | Powder feed, g/min | Carrier gas flow, L/min |
|---|---|---|---|---|---|---|---|
| A (1) | 5.2 | 1705 | 370 | 60° | One | 120 | 23 |
| B (6) | 5.8 | 1900 | 390 | 60° | One | 170 | 23 |
| C (10) | 5.8 | 2230 | 370 | 90° | One | 120 | 23 |
| D | 5.5 | 1960 | 380 | 90° | None | 150 | 26 |
| E | 5.2 | 2000 | 390 | 90° | None | 120 | 23 |
| F | 5.8 | 2230 | 390 | 90° | One | 120 | 29 |
| G | 5.2 | 2000 | 370 | 90° | None | 170 | 23 |

**Table 8 Summarized results of repeat and confirmation runs (Tables 6 and 7) using the agglomerated and sintered powder Porosity results obtained before repolishing are shown in parentheses. Other results from previous runs sprayed using the same parameters are shown in square brackets.**

| Test No. | Porosity, % | XRD(a) | Microstructure(b) | μm per pass | DE, % | Wear mass loss, mg | Wear rate, mg in 5 min |
|---|---|---|---|---|---|---|---|
| A1: Repeat 1 (A) | 0.80 (2.40) | 2 [7] | 4 [4] | 35 | 29 [42] | nd | nd |
| B1: Repeat 6 (K) | 0.90 (1.30) | 4 [4] | 3 [2] | 32 | 19 [21] | nd | nd |
| C1: Repeat 10 (L) | 0.35 (0.39) | 4 [2] | 3 [1] | 27 | 23 [30] | nd | nd |
| D1: Starting parameter | 0.12 (0.54) | 3 | 3 | 42 | 28 | 105 | 18 |
| E1: Best microstructure | 0.52 (1.15) | 2 | 2 | 36 | 30 | 125 | 24 |
| F1: Best XRD | 1.08 (0.95) | 2 | 3 | 21 | 17 | 85 | 16 |
| G1: Best DE | 0.71 (1.58) | 3 | 4 | 40 | 24 | 110 | 16 |
| Average runs D1-G1 | 0.64 (1.0) | 2.5 | 3 | 35 | 25 | 106 | 18.5 |

nd indicates not determined. (a) See Table 6 for XRD details. (b) Microstructures are ranked 1 to 5. 1 to 4 are acceptable.

**Table 9 Summary of the results obtained with the sintered and crushed powder, using the parameters listed in Tables 6 and 7 Porosity results obtained before repolishing are shown in parentheses.**

| Test No. | Porosity, % | XRD(a) | Microstructure(b) | μm per pass | DE, % | Wear mass loss, mg | Wear rate, mg in 5 min |
|---|---|---|---|---|---|---|---|
| A2 | 1.98 (1.03) | 2 | 5 | 52 | 43 | nd | ... |
| B2 | 0.59 (1.62) | 2 | 4-5 | 79 | 46 | nd | ... |
| C2 | 0.13 (1.94) | 1 | 4 | 55 | 46 | nd | ... |
| D2 | 1.70 (2.87) | 1 | 4-5 | 72 | 48 | 86 | 10 |
| E2 | 0.26 (2.49) | 1 | 4-5 | 62 | 52 | 87 | 13 |
| F2 | 1.58 (2.58) | 1 | 4-5 | 52 | 47 | 87 | 13 |
| G2 | 0.21 (2.31) | 1 | 4-5 | 71 | 42 | 100 | 16 |
| Average of D2-G2 | 0.9 (2.6) | 1 | 4.5 | 64 | 47 | 90 | 13 |

nd indicates not determined. (a) See Table 11. (b) Microstructures are ranked from 1 to 5. 1 to 4 are acceptable.

properties of these coatings. The differences in the DE, microstructure, and XRD curves of the coatings (within each powder type set) do not appear to correlate with the wear resistance. This is an important result in that it supports the hypothesis in section 3.3.3.

Further work as described in section 5, was performed to determine whether these variations in wear rate could be influenced by using a larger range of spray parameters or whether they are due mainly to the powder type and size.

## 5. Results of Further Work

### 5.1 *Samples Sprayed*

A series of coatings was produced using four sets of spray parameters, varying from those usually recommended by the gun manufacturer for low-melting point metals to those recommended for high-melting point alloys. The parameters were chosen to obtain as wide as possible a range of oxygen to kerosene flow ratios, without moving out of the parameter space typically recommended by the manufacturer of the equipment. Four powders were used. Tables 12 and 13 summarize the parameters used for these coatings, as well as the results obtained. The four parameters are listed in order of increasing oxygen to kerosene flow ratios.

### 5.2 *Abrasion Tests*

The samples were evaluated only in an abrasion test as described in section 2.1, since the primary aim was to see whether the powder type and the spray parameters have a large effect on the abrasion resistance. Each coating was deposited on two sam-

**Table 10 XRD results: repeat and confirmation runs using powder 1**

| Test No. | $W_2C$ | W | $CoC_x$ or $WC_{1-x}$ | Amorphous content ranking(a) |
|---|---|---|---|---|
| Repeat 1 | 2.1 | 2.9 | ... | 2 (7) |
| Repeat 6 | 2.2 | 2.0 | ... | 4 (4) |
| Repeat 10 | 2.2 | 2.2 | ... | 4 (2) |
| Starting parameter | <2 | <2 | <2 | 2 |
| | *4.5* | *4* | ... | *3* |
| Best microstructure | <2 | <2 | ... | 2 |
| | *3.9* | *3.1* | 2.8 | 2 |
| Best XRD | ≈1.0 | 2.8 | ... | 5 |
| Best DE | ≈1.2 | 1.3 | 2.4 | 3 |
| | *2.9* | *2.3* | *≈5* | *2* |

The same method as described for Table 4 was used. WC was always the major phase. Previous results for the same parameters are shown in parentheses. Results from the wear test samples that were sprayed with the same parameters are shown below the others in italics where applicable. (a) Where 0 is none and 8 is the highest amorphous content observed.

**Table 11 XRD results using the sintered and crushed powder**

| Test No. | $W_2C$ | W | $CoC_x$ or $WC_{1-x}$ | Amorphous content ranking(a) |
|---|---|---|---|---|
| 1 | 1.6 | <1 | ... | 2 |
| 6 | 7.4 | <1.5 | 3.5 | 2 |
| 10 | 1.7 | ... | ... | 1 |
| Starting parameter | 1.8 | ... | ... | 1 |
| | *5* | ... | *5* | *1* |
| Best microstructure | <1 | ... | ... | 1 |
| | *6.3* | ... | *4.5* | *1* |
| Best XRD | 1.4 | ... | ... | 1 |
| | *5* | ... | *3.7* | *1* |
| Best DE | <1 | ... | ... | 1 |
| | *8.3* | ... | *<4* | *1* |

The same method as described for Table 4 was used. WC was always the major phase. Results from wear test samples sprayed with the same parameters are shown below the others in italics, where applicable. (a) Where 0 is none and 8 is the highest amorphous content observed.

**Table 12 Wear test results from further work: WC-17% Co coatings**

| Run No. | Powder | Spray distance, mm | Kerosene flow, gph | $O_2$ flow, scfh | Total mass loss, mg | Steady-state wear rate, mg/5 min |
|---|---|---|---|---|---|---|
| Ag17/1 | Agglomerated 17%Co TAFA 1343V | 360 | 7.0 | 1700 | 80.0 | 14.4 |
| Ag17/2 | Agglomerated 17%Co TAFA 1343V | 380 | 6.2 | 2050 | 78.7 | 14.0 |
| Ag17/3 | Agglomerated 17%Co TAFA 1343V | 380 | 5.8 | 1950 | 101.3 | 16.7 |
| Ag17/4 | Agglomerated 17%Co TAFA 1343V | 360 | 5.0 | 1950 | 96.2 | 17.3 |
| Average for this group: | ... | ... | ... | ... | 89.1 | 15.6 |
| SC17/1 | Sintered crushed 17%Co WC-516 | 360 | 7.0 | 1700 | 78.5 | 12.9 |
| SC17/2 | Sintered crushed 17%Co WC-516 | 380 | 6.2 | 2050 | 72.8 | 12.4 |
| SC17/3 | Sintered crushed 17%Co WC-516 | 380 | 5.8 | 1950 | 72.6 | 12.3 |
| SC17/4 | Sintered crushed 17%Co WC-516 | 360 | 5.0 | 1950 | 76.4 | 12.8 |
| Average for this group: | ... | ... | ... | ... | 75.1 | 12.8 |

ples, and both were tested. The difference between the mass losses measured for the two samples in each case was ≤6% of their average mass loss, except for samples Ag12/2, Ag12/3, SC12/1, and Ag17/3, where the difference was between 8 and 13%. Hence, in the following discussions, any difference in mass loss of above 15% has been taken as significant when evaluating the results, while a difference of less than approximately 8% is seen as insignificant.

### 5.3 *Abrasion Rate of 12%Co Coatings*

With the exception of sample Ag12/1, the average mass loss for the WC 12%Co coatings was essentially identical for both powder types and for all parameters used. The steady-state wear rate, it appears that less oxidizing gas mixtures (lower oxygen to kerosene flow ratios) offer a slight wear rate advantage, but spray distance may also play a role. It appears that the spray parameters have a larger effect on the wear rate of the coatings produced using the agglomerated powder.

### 5.4 *Abrasion Rate of 17%Co Coatings*

The average mass loss for the agglomerated powders is significantly higher than that of the sintered and crushed powders, as is the variation from parameter to parameter. This confirms the previous results (section 4, a different batch of sand was used for the tests done in sections 4 and 5, which is why the results are not numerically identical). It appears that spray parameters have more of an effect on the coatings produced using agglomerated powder than on those produced from sintered and crushed powder. Therefore, for the two powders evaluated, the sintered powder provides both a lower wear rate and a more consistent property. This is probably due to morphology as well as size range differences. The effect of powder type and size is moreover more important than the effect of the spray parameter variations, which supports hypotheses in sections 3.3.3 and 3.3.4.

## 6. Conclusions

A Taguchi experimental design analysis was carried out to ascertain its suitability as a spray parameter optimization method for the spraying of WC 17%Co with a liquid fuel HP/HVOF system. The method could not be successfully applied to the liquid fuel HVOF process, and there was a large error term in the results of the statistical analyses. Several possible reasons for this were identified and tested by means of subsequent work. The following conclusions can be drawn from this work.

The microstructure, porosity, and phase composition of WC-17%Co HP/HVOF coatings produced using the JP-5000 system vary only slightly when the spray parameters are varied in the range shown in Table 1. These small variations cannot be correlated with the spray parameters used nor with the three-body

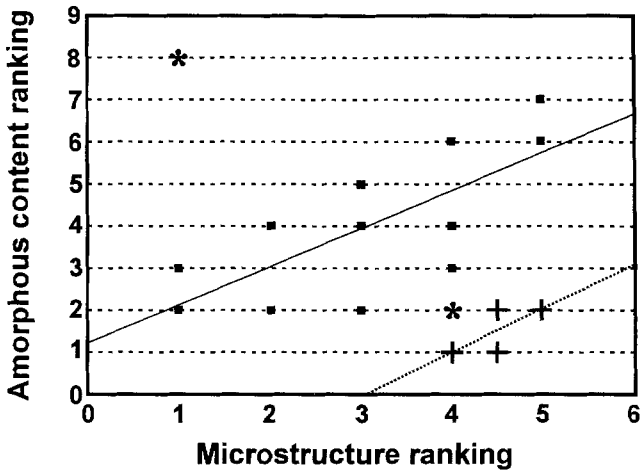


**Fig. 4** Correlation between the x-ray diffraction (XRD) and the microstructure results for coatings from agglomerated powders (■) and sintered powders (✚). The two points (✱) are also from the agglomerated powders but were disregarded when plotting the trend line.

**Table 13 Wear test results from further work: WC-12% Co coatings**

| Run No. | Powder | Spray distance, mm | Kerosene flow, gph | $O_2$ flow, scfh | Total mass loss, mg | Steady-state wear rate, mg/5 min |
|---|---|---|---|---|---|---|
| Ag12/1 | Agglomerated 12%Co WC-616 | 360 | 7.0 | 1700 | 41.4 | 6.3 |
| Ag12/2 | Agglomerated 12%Co WC-616 | 380 | 6.2 | 2050 | 49.9 | 7.1 |
| Ag12/3 | Agglomerated 12%Co WC-616 | 380 | 5.8 | 1950 | 52.1 | 7.2 |
| Ag12/4 | Agglomerated 12%Co WC-616 | 360 | 5.0 | 1950 | 51.8 | 7.6 |
| Average for this group: | ... | ... | ... | ... | 48.8 | 7.1 |
| SC12/1 | Sintered crushed 12%Co WC-489-1 | 360 | 7.0 | 1700 | 49.1 | 6.5 |
| SC12/2 | Sintered crushed 12%Co WC-489-1 | 380 | 6.2 | 2050 | 48.5 | 6.7 |
| SC12/3 | Sintered crushed 12%Co WC-489-1 | 380 | 5.8 | 1950 | 48.0 | 7.0 |
| SC12/4 | Sintered crushed 12%Co WC-489-1 | 360 | 5.0 | 1950 | 49.6 | 7.7 |
| Average for this group: | ... | ... | ... | ... | 48.8 | 7.0 |

abrasion resistance of the coatings. These variations are probably insignificant.

The JP-5000 HP/HVOF process is very robust for spraying WC-Co coatings, because when the spray parameters are changed within a large parameter space while keeping the powder type constant, the three-body abrasion resistance of coatings does not vary by more than approximately 20% in the worst case observed, and usually by not more than approximately 8%. The powder type and size appear to have a more significant influence on wear rate than the spray parameters themselves. Thus, the initial approach used for the Taguchi method, which assumed that small parameter variations would have a significant effect, did not work. It also implies that costly attempts at parameter optimization are not necessary for this spray system when spraying WC-Co coatings.

The average abrasion rate of the two WC-12%Co coating types tested is approximately two-thirds that of the best WC-17%Co coating type tested.

In the case of the 17%Co coatings, the sintered and crushed powder delivered a more consistent and a lower wear rate than the agglomerated and densified powder type, but this effect was possibly related more to the powder size than to its manufacturing route.

A correlation was found between the microstructure and the amorphous content for the 17%Co coatings produced. As the amorphous phase content in the coatings increased, the quality of the microstructure tended to deteriorate. The microstructures from the sintered and crushed powders were generally inferior, but their XRD and wear results were better than those of the other coatings.

## Acknowledgments

The authors would like to thank Professor Silvana Luyckx, Dr. Danie de Wet, and Hugo Howse for reviewing this paper. In addition, the authors thank Jan Kinds, Philip van Wyk, and Heide Snyders for assisting with the powder and coating characterization work. Also, thanks are extended to Piet Terblanche for advice on interpreting the XRD results.

## References

1. R. Kingswell, K.T. Scott, and L.L. Wassell, Optimizing the Vacuum Plasma Spray Deposition of Metal, Ceramic, and Cermet Coatings using Designed Experiments, *Thermal Spray: International Advances in Coatings Technology,* C.C. Berndt, Ed., ASM International, 1992, p 421-426
2. T.C. Nerz, J.E. Nerz, B.A. Kushner, and A.J. Rotolico, Evaluation of HEP Sprayed Tungsten Carbide/Cobalt Coating using Design of Experiment Method, *Thermal Spray: International Advances in Coatings Technology,* C.C. Berndt, Ed., ASM International, 1992, p 402-414
3. D.J. Varacalle, G.R. Smolik, G.C. Wilson, G. Irons, and J.A. Walter, An Evaluation of Tungsten Carbide-Cobalt Coatings Fabricated with the Plasma Spray Process, *Protective Coatings: Processing and Characterization,* R.M. Yazici, Ed., The Minerals, Metals, and Materials Society, 1990, p 121-134
4. T.J. Steeper, D.J. Varacalle, G.C. Wilson, W.L. Riggs, A.J. Rotolico, and J.E. Nerz, A Design of Experiment Study of Plasma Sprayed Alumina-Titania Coatings, *Thermal Spray: International Advances in Coatings Technology,* C.C. Berndt, Ed., ASM International, 1992, p 415-420
5. W.L. Riggs, R.K. Betz, and N. Jayaraman, Taguchi Experimental Design Study of Plasma and HVOF Chrome Carbide/Nickel Chromium, *Thermal Spray Research and Applications,* T.F. Bernecki, Ed., ASM International, 1991, p 711-728
6. J. Walter and W.L. Riggs, Plasma Spray Coating Parameter Development, *Thermal Spray Research and Applications,* T.F. Bernecki, Ed., ASM International, 1991, p 729-733
7. H.E. Exner et al., *Prakt. Metallogr.,* Vol 30, 1996, p 322
8. K. Korpiola and P. Vuoristo, Effect of HVOF Gas Velocity and Fuel to Oxygen Ratio on the Wear Properties of Tungsten Carbide Coating, *Thermal Spray: Practical Solutions for Engineering Problems,* C.C. Berndt, Ed., ASM International, 1996, p 177-184
9. H.L. de Villiers Filmer and A.J. Jurriaanse, *The Influence of Starting Powder Properties on the Structure and Wear Behaviour of WC-Co Thermal Spray Coatings,* Report No., WBS 131-02, MATTEK, Project No. MMM1R/029, CSIR, Pretoria, South Africa, 1996
10. J.E. Nerz, B.A. Kushner, and A.J. Rotolico, Effects of Deposition Methods on the Physical Properties of Tungsten Carbide-12 wt% Cobalt Thermal Spray Coatings, *Protective Coatings: Processing and Characterization,* R.M. Yazici, Ed., The Minerals, Metals, and Materials Society, 1990, p 135-143
11. C.-J. Li, A. Ohmori, and Y. Harada, Effect of Powder Structure on the Structure of Thermally Sprayed WC-Co Coatings, *J. Mater. Sci.,* Vol 31, 1996, p 785-794
12. J. R. Fincke, W. D. Swank, and D.C. Haggard, Comparison of the Characteristics of HVOF and Plasma Thermal Spray, *Thermal Spray Industrial Applications,* C.C. Berndt and S. Sampath, Ed., ASM International, 1994, p 325-330
13. J. Subrahmanyam, M.P. Srivastava, and R. Sivakumar, Characterization of Plasma Sprayed WC-Co Coatings, *Mater. Sci. Eng.,* Vol 84, 1986, p 209-214
14. Ch. Heinzelmaier and K.K. Schweitzer, WC-Co Coatings for Protection Against Hammer Wear in Flight Engines, *Proc. Therm. Spray Conf. TS90,* (Essen, Germany, August 1990), Deutsche Verband für Schweisstechnik, Düsseldorf, publication No. DVS 130, 1990, p 51-54
15. J.E. Nerz, B.A. Kushner, and A.J. Rotolico, Microstructural Evaluation of Tungsten Carbide-Cobalt Coatings, *J. Therm. Spray. Technol.,* Vol 1, 1992, p 147-152
16. A. Karimi, Ch. Verdon, and G. Barbezat, Microstructure and Hydroabrasive Wear Behaviour of High Velocity Oxy-Fuel Thermally Sprayed WC-Co(Cr) Coatings, *Surf. Coat. Technol.,* Vol 57, 1993, p 81-89
17. Ch. Verdon, *Microstructure et Résistance à l'Érosion de Revêtements WC-M Déposés par Projection Thermique HVOF (French),* Ph.D. thesis No. 1393, École Polytechnique Fédérale de Lausanne (EPFL), Switzerland, 1995
18. L.E. McCandlish, B.H. Kear, B.K. Kim, and L.W. Wu, Low Pressure Plasma Sprayed Coatings of Nanophase WC-Co, *Protective Coatings: Processing and Characterization,* R.M. Yazici, Ed., The Minerals, Metals, and Materials Society, Warrendale, PA, 1990, p 113-119
19. C.J. Li, A. Ohmori, and Y. Harada, Formation of an Amorphous Phase in Thermally Sprayed WC-Co, *J. Therm. Spray Technol.,* Vol 5 (No. 1), 1996, p 69-73
20. J.E. Nerz, B.A. Kushner, and A.J. Rotolico, Characterization of Tungsten Carbide Coatings as a Function of Powder Manufacturing and Deposition Technologies, *Mater. Sci. Monogr. (High Performance Ceramic Films and Coatings),* Vol 67, 1991, p 27-36
21. B.A. Detering, J.R. Knibloe, and T.L. Eddy, Occurrence of Tungsten Plasma in Plasma Spraying of WC/Co, *Thermal Spray Research and Applications,* T.F. Bernecki, Ed., ASM International, 1991, p 27-31
22. G. Barbezat, E. Müller, and B. Walser, Metallurgische Aspekte und Eigenschaften von Wolframkarbid-Kobalt-Schichten hergestellt mit dem KET KOTE Verfahren (in German), *VDI-Berichte,* Vol 670, 1988, p 853-872

23. J.E. Nerz, B.A. Kushner, and A.J. Rotolico, Effects of Deposition Methods on the Physical Properties of Tungsten Carbide-12 wt% Cobalt Thermal Spray Coatings, *Protective Coatings: Processing and Characterization,* R.M. Yazici, Ed., The Metals and Minerals Society, 1990, p 135-143
24. T.P. Slavin and J. Nerz, Material Characteristics and Performance of WC-Co Wear Resistant Coatings, *Thermal Spray Research and Applications,* T.F. Bernecki, Ed., ASM International, 1991, p 159-165
25. P. Vuoristo, K. Niemi, A. Mäkelä, and T. Mäntylä, Spray Parameter Effects on Structure and Wear Properties of Detonation Gun Sprayed WC + 17%Co Coatings, *Thermal Spray: Research, Design, and Applications,* C.C. Berndt and T.F. Bernecki, Ed., ASM International, 1993, p 173-178
26. M.S.A. Khan and T.W. Clyne, Microstructure and Abrasion Resistance of Plasma Sprayed Cermet Coatings, *Thermal Spray: Practical Solutions for Engineering Problems,* C.C. Berndt, Ed., ASM International, 1996, p 113-122
27. W.J. Lenling, M.F. Smith, and J.A. Henfling, Process for Producing Plasma Sprayed Carbide-Based Coatings with Minimal Decarburization and Near Theoretical Density, *Thermal Spray Research and Applications,* T.F. Bernecki, Ed., ASM International, 1991, p 451-455
28. A. Karimi and C. Verdon, Hydroabrasive Wear Behaviour of High Velocity Oxyfuel Thermally Sprayed WC-M Coatings, *Surf. Coat. Technol.,* Vol 62, 1993, p 493-498
29. P.L. Kuhanen and P.O. Kettunen, Comparison of Plasma and Detonation Gun Sprayed Tungsten Carbide-Cobalt Coatings, *Proc. Therm. Spray. Conf. TS93, Aachen, Germany, 3-5 March 1993,* Pub. Deutsche Verband für Schweisstechnik, Düsseldorf, Publication No. DVS 152, 1993, p 100-102